



HAL
open science

A Multiscale Approach to Predict Classical Losses in Soft Magnetic Composites

Adelina Bordianu, Olivier de La Barrière, Oriano Bottauscio, Alessandra Manzin, Mario Chiampi

► **To cite this version:**

Adelina Bordianu, Olivier de La Barrière, Oriano Bottauscio, Alessandra Manzin, Mario Chiampi. A Multiscale Approach to Predict Classical Losses in Soft Magnetic Composites. *IEEE Transactions on Magnetics*, 2013, 48 (4), pp. 1537 - 1540. hal-00825526

HAL Id: hal-00825526

<https://hal.science/hal-00825526>

Submitted on 24 May 2013

HAL is a multi-disciplinary open access archive for the deposit and dissemination of scientific research documents, whether they are published or not. The documents may come from teaching and research institutions in France or abroad, or from public or private research centers.

L'archive ouverte pluridisciplinaire **HAL**, est destinée au dépôt et à la diffusion de documents scientifiques de niveau recherche, publiés ou non, émanant des établissements d'enseignement et de recherche français ou étrangers, des laboratoires publics ou privés.

A Multiscale Approach to Predict Classical Losses in Soft Magnetic Composites

Adelina (Samoilescu) Bordianu¹, Olivier de la Barrière², Oriano Bottauscio², Mario Chiampi³, and
Alessandra Manzin²

¹Electrical Engineering Department, University "Politehnica" of Bucharest, Bucharest RO-060042, Romania

²Istituto Nazionale di Ricerca Metrologica (INRIM), Torino I-10135, Italy

³Dipartimento di Ingegneria Elettrica, Politecnico di Torino, Torino I-10129, Italy

This paper presents the application of a finite element multiscale method, based on the homogenization technique, to the prediction of classical losses in soft magnetic composite materials. The experimental results, obtained for a wide range of frequencies and for various toroidal samples with different cross sections, are explained by using the considered model. It has been found that the classical losses are influenced by the dimensions of the sample, as well as by the conductivity and the length of the random contacts between the grains.

Index Terms — Composite materials, numerical analysis, multiscale problem, classical losses.

I. INTRODUCTION

SOFT MAGNETIC Composites (SMC) appear as very promising in many industrial applications, as for example in high speed electrical machines [1]. Indeed, their granular structure leads to a significant reduction of the classical loss contribution, which, however, can become important at the frequency increase [2]. Moreover, unlike conventional laminated materials, SMC exhibit isotropic magnetic properties, which can make them suitable in machines with 3D flux paths, such as axial flux machines [3]. They also possess isotropic thermal properties [4], which is an important feature for loss dissipation.

An accurate loss prediction is essential for a reliable optimization of electrical machines using such materials. Since the classical loss gives the most important contribution in high frequency applications, this paper focuses on a modeling approach for the computation of eddy currents in SMC materials.

SMC are composed of grains made of a magnetic material (often pure iron). The grains are resin-insulated from each other and then compressed under high pressure. During the compaction, random contacts can appear between grains, as pointed out in [5]. These random contacts are responsible for a SMC bulk conductivity, which is much lower than the one of the grains, but not negligible, giving rise to eddy current circulation at macroscopic scale (sample size).

A model for computing the SMC equivalent permeability taking into account the grain contacts has been proposed in [6]. Here, a micrograph image is exported to an electromagnetic finite element software and used to deduce an equivalent permeability, which is found in good agreement with the measurements. Such an approach could be extended also to eddy current computations, but it is

limited to very small samples because of the huge number of mesh elements required for a reliable discretization. Other authors have analyzed so small samples that the effects of current paths flowing from grain to grain at the sample scale are negligible [7]. Only the microscopic eddy currents flowing at the grain scale have been taken into account, considering rectangular grains. However, this simplifying assumption is usually not verified in electrical machine applications, where non negligible intergrain currents are present. Therefore, in [8] the classical loss contribution has been evaluated by introducing a loss decomposition into two terms: the first one is due to the eddy currents at the grain scale, the second one is related to the eddy currents at the macroscopic scale and linked to the bulk resistivity. However, this loss summation is not straightforward from a mathematical point of view.

This paper proposes the use of a method based on a multi-scale homogenization technique [9], successfully applied to different non-homogeneous materials, such as ferrites [10]. The main difficulty encountered here is to model the random contacts between grains using the homogenization method. In the first part of the paper, the experimental evidence of the macroscopic eddy currents is shown. Then, the idealized model of the contacts between grains, to be used in the homogenization process, is introduced. The last part of the paper presents the comparison between the experimental results and the model.

II. EXPERIMENTS

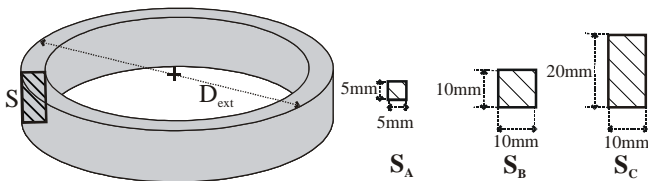
The presence of macroscopic eddy currents flowing from grain to grain at the sample scale is put in evidence in this section. This evidence is based on the remark that only the macroscopic eddy current term, unlike the loss contributions at the grain scale (hysteresis, excess, and local eddy currents), can be responsible for a dependence of the specific loss on the sample size and shape. The analysis presented in

88 [7] shows that a toroid with a square cross section $S = 5 \times 5$
 89 mm^2 seems to be small enough to neglect macroscopic eddy
 90 currents. Indeed, when decreasing the section to 2.5×2.5
 91 mm^2 , a negligible change in the specific loss has been
 92 observed. Here, the analysis is centered on toroids with cross
 93 sections greater than $5 \times 5 \text{ mm}^2$, where not negligible
 94 macroscopic eddy currents are expected.

95 **A. Description of the experimental set-up**

96 The considered SMC are produced by the Swedish
 97 company Höganäs in bulk cylindrical shape (diameter: 80
 98 mm, height: 20 mm), under the reference “Prototyping” [11].
 99 Since these blocks can be quite easily cut, they are well
 100 suitable for making toroids of different cross sections, as the
 101 ones investigated in this paper and represented in Fig. 1. The
 102 first section (toroid A: $S_A = 5 \times 5 \text{ mm}^2$) is considered as the
 103 reference case [7], having assumed that the eddy currents are
 104 confined at the grain scale. Two larger samples are also
 105 considered: toroid B ($S_B = 10 \times 10 \text{ mm}^2$) and toroid C ($S_C =$
 106 $10 \times 20 \text{ mm}^2$). The external diameter D_{ext} of the toroids is
 107 always set at its maximal value (i.e. the external diameter of
 108 the blocks, equal to 80 mm), in order to ensure a uniform
 109 flux density distribution throughout the entire cross section.

110 It is also important to give some details about the cutting
 111 procedure. Indeed, some authors [12] have pointed out the
 112 fact that a mechanical abrasion could create conductive paths
 113 on the material surface. This could introduce criticalities in
 114 our experiments: if the four faces of the toroid are made
 115 conductive by the cutting abrasion, a fictitious closed
 116 electrical turn would be created on the toroid surface. This is
 117 another reason why the toroids have an external diameter
 118 equal to the external diameter of the blocs $D_{ext} = 80\text{mm}$. This
 119 choice ensures that at least the external face has not
 120 undergone any abrasion, therefore making impossible the
 121 formation of a closed conductive turn around the toroids.

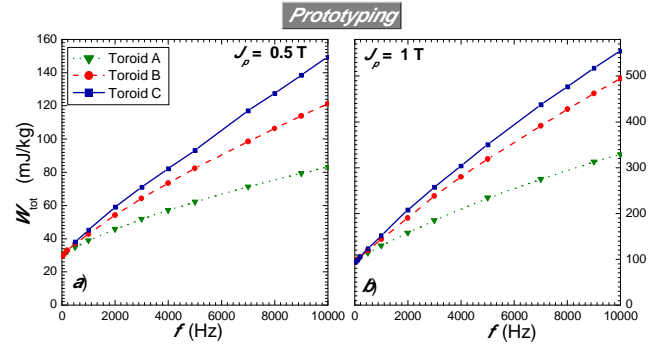


122 Fig. 1. Scheme of the toroidal sample and of the different cross sections
 123 considered in the analysis.
 124

125 The experimental loss measurement is carried out as
 126 follows. The toroid is wound by two windings. The primary
 127 winding is supplied under AC conditions with a linear power
 128 amplifier. The current flowing in this primary winding is
 129 measured using a resistive sensor. This allows to deduce the
 130 applied magnetic field, which is, according to Ampere’s law,
 131 proportional to the current. The mean flux density over the
 132 toroid cross section is measured by the integration of the
 133 voltage given by a secondary winding. Then, the $B-H$ curve
 134 is deduced, and the area of the cycle gives the total specific
 135 loss per cycle W_{tot} . A feedback loop permits to get a perfect
 136 sinusoidal polarization in the toroid, assumed to be equal to
 137 the magnetic flux density (frequency f , peak value J_p).

138 **B. Loss results in the different toroids**

139 The total specific energy loss per cycle $W_{tot}(J_p, f)$ measured
 140 in the considered toroids are given in Fig. 2. The dependence
 141 of the specific loss on the toroid cross section due to
 142 macroscopic eddy current patterns is well evident.

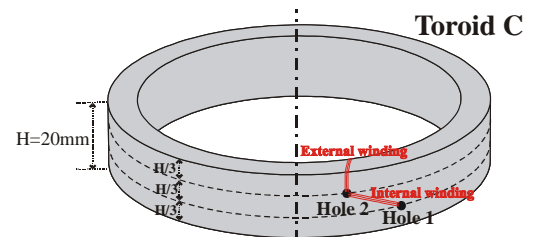


143 Fig. 2. Total measured loss $W_{tot}(J_p, f)$ versus frequency f for $J_p=0.5\text{T}$ (a) and
 144 $J_p=1\text{T}$ (b).
 145

146 **C. Assumption of no skin effect for the loss separation**

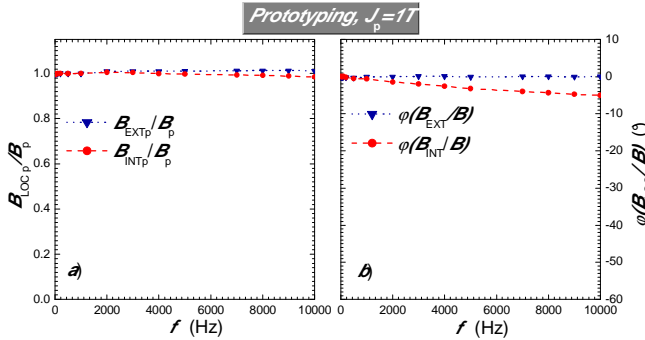
147 The loss separation has been carried out following the
 148 approach described in [7]. Starting from the assumption of
 149 only local eddy currents in toroid A, a model of eddy
 150 currents at the scale of the single grain has been developed.
 151 The hysteresis and excess losses, which are local per
 152 definition, have been extracted. Then, we assume that, under
 153 the same excitation conditions (frequency f and polarization
 154 peak value J_p), the excess and hysteresis losses in toroids B
 155 and C are equal to the ones in toroid A, in spite of the
 156 presence of macroscopic eddy currents which change the
 157 classical loss. Therefore, the classical loss contribution in
 158 toroids B and C is computed by subtracting hysteresis and
 159 excess loss obtained in toroid A from the total measured loss.

160 This procedure is valid if we assume that the macroscopic
 161 eddy current patterns do not modify the local magnetic flux
 162 density in the toroid. In other terms, the skin effect at the
 163 sample scale must be negligible. To verify this assumption
 164 experimentally the local magnetic flux density in the cross
 165 section of toroid C has been measured, by drilling two holes
 166 in the toroid, as represented in Fig. 3. An internal coil
 167 between the two holes allows us the measurement of the
 168 internal magnetic flux density $B_{int}(t)$, while an external
 169 winding enables the detection of the external field $B_{ext}(t)$.
 170 The skin effect due to macroscopic eddy current patterns is
 171 negligible if these internal and external magnetic flux density
 172 components do not differ from the mean field $B(t)$ measured
 173 at the secondary winding.



174 Fig. 3. Scheme of the measurement procedure for the internal and external
 175 magnetic flux density components in toroid C.
 176

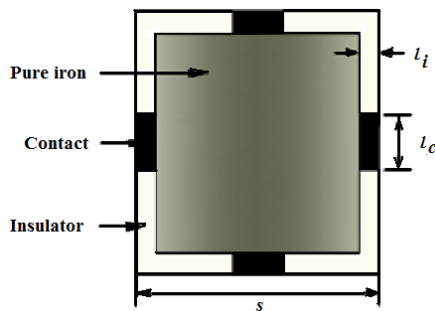
177 The ratios of the peak values of the local and mean
 178 magnetic flux densities and the phase shift between their first
 179 harmonics are plotted versus frequency for $J_p=1$ T in Fig.
 180 4(a) and in Fig. 4(b), respectively. The amplitude of the ratio
 181 is close to unity, while the phase shift does not exceed 5° , so
 182 that the assumption of negligible skin effect is well justified.



183 Fig. 4. a) Ratios of the peak values of the local magnetic flux densities,
 184 $B_{ext}(t)$ and $B_{int}(t)$, and the mean magnetic flux density $B(t)$. b) Phase shifts
 185 between the first harmonics of the local and mean magnetic flux densities.
 186

187 III. MODELING APPROACH

188 The starting point of the modeling approach is the
 189 application of the mathematical homogenization technique to
 190 infer the physical and geometrical properties of the
 191 equivalent contacts between the grains. For such a purpose,
 192 the 3D random distribution of grains, with possible contacts,
 193 is replaced with a 2D periodic structure represented by the
 194 repetition of an idealized elementary cell. A known
 195 sinusoidal magnetic flux is imposed along the direction
 196 normal to this 2D domain and the electromagnetic field
 197 problem is formulated in terms of an electric vector potential
 198 with homogeneous Dirichlet boundary conditions [13]. The
 199 governing equation is written in the frequency domain
 200 expressing the field quantities as phasors. All the field
 201 problems involved in the adopted approach are solved
 202 through the Finite Element Method.



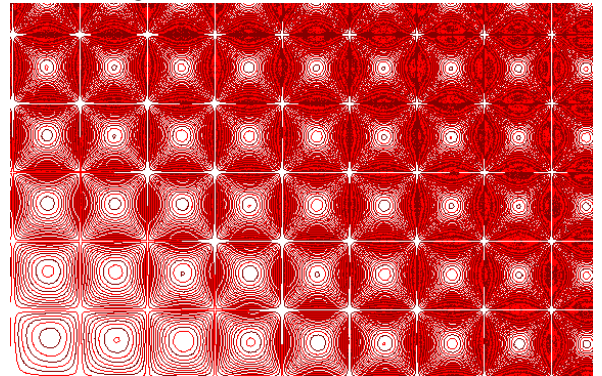
203 Fig. 5: Scheme of the elementary cell with idealized grain contacts.
 204

205 For the specific application, the elementary square cell ($s =$
 206 $115 \mu\text{m}$) shown in Fig. 5 is adopted, where four regions
 207 connecting the surrounding cells are introduced to simulate
 208 the presence of grain contacts. The idealized square grain
 209 is assumed to have the average dimensions of the actual grains,
 210 observed in the micrograph images.

211 Both for grain and contacts the relative magnetic
 212 permeability is assumed to be equal to 450, as deduced by a

213 3D analysis. However, the precise value of this parameter
 214 has a limited impact, due to the absence of skin effect shown
 215 in the previous section. The grain is made of pure iron with
 216 an electrical conductivity of 10 MS/m . The non-magnetic
 217 insulating layer has a thickness $l_i = 0.74 \mu\text{m}$ and a high
 218 resistivity ($\rho_i = 10 \text{ M}\Omega\text{m}$). The length and the electrical
 219 conductivity of the contact are chosen, by a trial and error
 220 procedure, to fit the classical loss contribution. Magnetic
 221 fluxes Φ corresponding to uniform magnetic flux densities of
 222 0.5 T and 1 T are imposed along the direction normal to the
 223 sample cross-section.

224 Since the aim is an accurate evaluation of the classical
 225 losses at both grain and sample scales, a multiscale model
 226 able to reconstruct the macroscopic and local distribution of
 227 eddy currents has to be adopted. The mathematical
 228 homogenization approach, based on the multiple scale
 229 expansion theory [13], is suitable for this application. Indeed,
 230 following this technique, the field equation is handled by
 231 searching a solution expressed in an asymptotic form, with a
 232 zero-order term and higher-order correctors. The first term
 233 describes the homogenized solution computed in a
 234 homogenous medium with "average" properties; the other
 235 terms introduce corrections to reproduce the local behavior
 236 of the heterogeneous material. A detailed description of the
 237 mathematical formulation can be found in [9]. As an
 238 example, the effect of the superimposition of the local terms
 239 to the global one is shown in the eddy current distribution
 240 presented in Fig. 6.



241
 242 Fig.6. Distribution of current field lines in the cross section of a SMC toroid,
 243 computed using the homogenization method with second order correctors.

244 IV. RESULT DISCUSSION

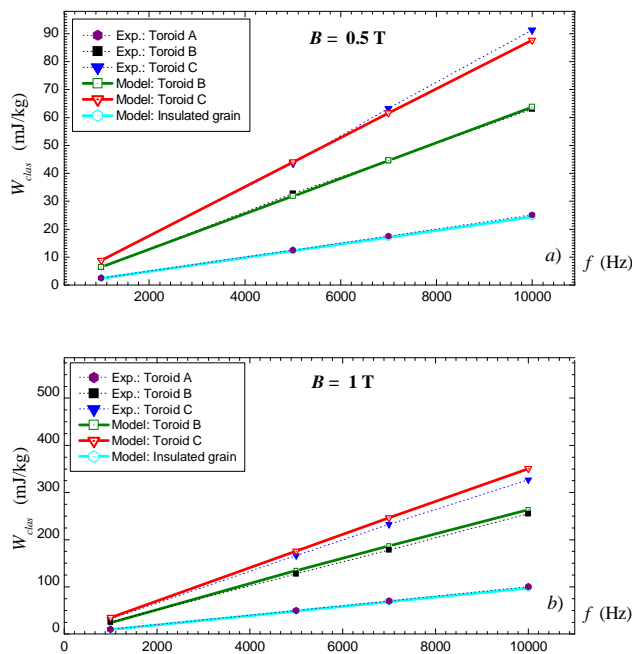
245 The first problem for the model development is the
 246 characterization of the contact, starting from the
 247 experimental data. Having fixed the insulating layer
 248 thickness, two parameters have to be identified: the contact
 249 length l_c and its conductivity σ_c . To investigate the influence
 250 of these parameters on the classical loss component, l_c is
 251 varied from $\sim 0.025 \mu\text{m}$ up to $115 \mu\text{m}$ (full contact) and σ_c is
 252 varied in the range between $\sim 20 \text{ S/m}$ and $\sim 100000 \text{ S/m}$.

253 A first analysis, performed keeping constant one of the
 254 two parameters, shows that the increase of the other one
 255 always leads to an increase in the macroscopic eddy currents
 256 and in the classical loss too. However, when the two

257 parameters are simultaneously modified maintaining their
 258 product constant, the classical loss remains practically
 259 unchanged in the whole range of contact length. This implies
 260 that a single parameter (the product $\sigma_c l_c$) can fully identify
 261 the properties of the contact.

262 The identification process is performed considering the
 263 total loss measured in toroid B at 7000 Hz from which the
 264 hysteresis and excess losses obtained in toroid A are
 265 subtracted to evaluate the classical loss contribution. A value
 266 of 2850 S has been determined for the product $\sigma_c l_c$ and
 267 adopted in all the simulations carried out in the frequency
 268 range from 1 kHz to 10 kHz, where the SMC components
 269 usually operate and the influence of eddy currents is better
 270 highlighted.

271 The comparison between the experimental and computed
 272 classical losses in toroids B and C are presented in Fig. 7 for
 273 two flux values, corresponding respectively to uniform flux
 274 densities of 0.5 T and 1.0 T.
 275



276 Fig. 7. Classical losses W_{clas} as a function of frequency f , for a magnetic flux
 277 density of 0.5T (a) and 1 T(b)
 278

279 For the both toroids the model provides results in very
 280 good agreement with the experiments. The relative error is
 281 less than 3% for a magnetic flux density of 0.5 T and it is
 282 approximately 6% for 1 T. The errors can be attributed both
 283 to the measurement uncertainty and to the approximations
 284 intrinsic in a numerical model. The greater errors in the 1 T
 285 case can be explained by the higher temperature increase in
 286 the sample, consequent to the loss enhancement, which can
 287 modify the material properties. For both sections, the
 288 influence of macroscopic eddy currents cannot be
 289 disregarded and it is responsible of the dependence of the
 290 classical losses on the sample size. For toroid A, a good
 291 agreement with the numerical model is also found when
 292 simulating insulated grains (i.e. the circulation of
 293 macroscopic grains is neglected).

V. CONCLUSION

294 The paper proposes a computational method, based on a
 295 multi-scale homogenization technique, for the evaluation of
 296 the classical loss component in composite materials. The
 297 model takes into account the presence of macroscopic eddy
 298 currents, which can flow between grains due to random
 299 contacts. The comparison between the experimental and
 300 numerical results shows a good agreement for toroids with
 301 large cross sections. It has been observed that at the increase
 302 of the toroid size the current path, which is mainly local for
 303 small cross sections, tends towards a more global
 304 distribution.

305 The proposed model is able to evaluate the increase of the
 306 classical loss due to the presence of currents at sample scale
 307 for any kind of SMC materials, provided that some
 308 measurements are available for the material identification.
 309

ACKNOWLEDGMENT

310 Mrs. Adelina (Samoilescu) Bordianu work has been
 311 funded by the Sectoral Operational Programme Human
 312 Resources Development 2007-2013 of the Romanian
 313 Ministry of Labour, Family and Social Protection through the
 314 Financial Agreement POSDRU/88/1.5/S/60203.
 315

REFERENCES

- 316 [1] A. Chebak, P. Viarouge, and J. Cros, "Analytical Computation of the
 317 Full Load Magnetic Losses in the Soft Magnetic Composite Stator of
 318 High-Speed Slotless Permanent Magnet Machines," *IEEE Trans. Magn.*, vol. 45, no. 3, pp. 952-955, 2009.
 319 [2] J. Wang, T. Ibrahim, and D. Howe, "Prediction and Measurement of
 320 Iron Loss in a Short-Stroke, Single-Phase, Tubular Permanent Magnet
 321 Machine," *IEEE Trans. Magn.*, vol. 46, no. 6, pp. 1315-1318, 2010.
 322 [3] G.S. Liew, N. Ertugrul, W.L. Soong, and D.B. Gehlert, "Analysis and
 323 Performance Evaluation of an Axial-Field Brushless PM Machine
 324 Utilising Soft Magnetic Composites," in *IEEE Int. Conf. on Electric
 325 Machines & Drives*, Antalya, 2007, pp. 153-158.
 326 [4] F. Marignetti and V.D. Colli, "Thermal Analysis of an Axial Flux
 327 Permanent-Magnet Synchronous Machine," *IEEE Trans. Magn.*, vol.
 328 45, no. 7, pp. 2970-2975, 2009.
 329 [5] C. Yanhong and GB. Kliman, "Modeling of soft magnetic
 330 composites," in *IEEE Industry Applications Conf. (IAS)*, 2004.
 331 [6] C Cyr, P. Viarouge, S. Clénet, and J. Cros, "Methodology to Study
 332 the Influence of the Microscopic Structure of Soft Magnetic
 333 Composites on Their Global Magnetization Curve," *IEEE Trans. Magn.*,
 334 vol. 45, no. 3, pp. 1178-1181, 2009.
 335 [7] O. de la Barrière et al., "Loss separation in soft magnetic composites,"
 336 *J. Appl. Phys.*, vol. 109, p. 07A317, 2011.
 337 [8] D. Zidaric, B. Zagirnyak, and M. Miljavec, "Soft magnetic composite
 338 in design of BLDC motor," in *Int. Conf. on Electrical Machines*,
 339 Cracow, 2004.
 340 [9] O. Bottauscio, A. Manzin, V.C. Piat, M. Codegone, and M. Chiampi,
 341 "Electromagnetic phenomena in heterogeneous media: Effective
 342 properties and local behavior," *J. Appl. Phys.*, vol. 100, p. 044902,
 343 2006.
 344 [10] F. Fiorillo, C. Beatrice, O. Bottauscio, A. Manzin, and M. Chiampi,
 345 "Approach to magnetic losses and their frequency dependence in Mn-
 346 Zn ferrites," *Appl. Phys. Lett.*, vol. 89, no. 12, pp. 122513.1-3, 2006.
 347 [11] Höganäs SMC Brochures. [Online].
 348 <http://www.hoganas.com/en/Products--Applications/Soft-Magnetic-Composites/SMC-Brochures-Pics/>
 349 [12] C. Cyr, P. Viarouge, J. Cros, S. Clénet, "Resistivity measurement on
 350 soft magnetic composite materials," *Przeglad Elektrotechniczny*, vol.
 351 83, no. 4, pp. 103-104, 2007.
 352 [13] O. Bottauscio, M. Chiampi, and A. Manzin, "Determination of the
 353 electromagnetic properties in magnetic composite materials by
 354 inverse homogenisation," *J. Magn. Magn. Mat.*, vol. 320, pp. e547-
 355 e550, 2008.
 356
 357
 358